An Ab Initio Study of Structure and Energetics of Free-Base Bonellin-Dimethylester Isomers and Transition States

Dage Sundholm,*[a] Henrik Konschin,[a] and Marco Häser[b]

In memory of Dr. Marco Häser, who died tragically in a climbing accident in August 1997

Abstract: The molecular structures of bonellin-dimethylester isomers and transition states, for the hydrogen migration of the inner hydrogens, have been optimized at density functional level by the use of split-valence basis sets augmented with polarization functions. Accurate values for the relative energies of the six isomers and the eight transition states have been obtained by performing second-order Møller–Plesset calculations. The isomer energies obtained at density functional level are 2–5 kcal mol^{-1} smaller than second-order Møller–Plesset values, while the isomer energies calculated at Hartree–Fock level are typically 1 kcal mol^{-1} too small compared with second-order Møller–Plesset values, except for one isomer whose Hartree–Fock energy is 7 kcal mol^{-1} larger. Compared with the second-order Møller–Plesset values, the energy barriers for the transition between the isomers calculated at density functional level are 3–7 kcal mol^{-1} too small, whereas those obtained at Hartree–Fock level are 6–8 kcal mol^{-1} too large. Nuclear magnetic shielding constants calculated at Hartree–Fock level are also reported. The calculated nuclear magnetic shieldings are used for analyzing the aromaticity and the aromatic pathway of the porphyrin nucleus.

Keywords: ab initio calculations · aromaticity · porphyrin · proton migration · tautomerism · transition states

Introduction

The tautomeric exchange involving inner hydrogen migration is a fundamental property of porphyrins; this has been the subject of extensive experimental and computational studies.[1–13] Computational studies at ab initio level have so far mostly been restricted to unsubstituted free-base porphyrins ($PorH_2$) and monodeprotonated free-base porphyrin ($PorH^-$). A number of studies have focused on computational method assessment,[14–16] spectral details,[17–20] force fields,[21–23] and substituent effects[24–28] of porphyrins. Recently Ghosh and Jynge have made extensive local density functional (LDF) calculations on the *cis*–*trans* isomerism in porphyrin isomers[29] and they also compared free-base porphyrin with various chlorins.[30]

In this work we apply ab initio methods on bonellin-dimethylester, which is a multiply substituted free-base porphyrin possessing C_1 symmetry. Since all substituents are different, six nondegenerate isomers are obtained by permuting the inner hydrogens and the eight transition states (with one imaginary vibrational frequency) of the migration of the inner hydrogens. Bonellin is the green pigment of Bonellia viridis (a marine animal in the Mediterranean[31]) that is secreted upon irritation. Bonellin stunts the growth of the sexually undifferentiated larvae and is responsible for their development into the male gender. It exhibits antibiotic[32] and antitumour[33] characteristics in vitro, and has therefore captured the interest of both chemists and biologists.[31–37]

The absolute configuration of bonellin has recently been established experimentally and its dimethylester has been synthesized from four monocyclic building blocks.[35, 36] Bonellin-dimethylester has also been the subject of extensive nuclear magnetic resonance studies.[37] The NMR spectrum possesses fine structure at low temperature due to nonequivalent free-base hydrogens, while at room temperature only one free-base hydrogen NMR resonance is found. These intriguing observations led to the present calculations as a means of predicting possible isomers.

[a] Prof. D. Sundholm, H. Konschin
Department of Chemistry, PO Box 55 (A. I. Virtasen aukio 1)
FIN-00014 Helsinki (Finland)
Fax: (+385) 9-19140169
E-mail: sundholm@chem.helsinki.fi

[b] Dr. M. Häser
Lehrstuhl für Theoretische Chemie, Institut für Physikalische Chemie
Universität Karlsruhe, D-76128 Karlsruhe (Germany)

Computational methods

In density functional theory (DFT) methods, the exchange correlation term is approximated by a function of the electron density [$\rho(r)$] and its gradient [$\Delta\rho(r)$]. In this way one achieves a separation of the evaluation of the Coulomb and exchange-correlation terms, which opens the way to a more efficient treatment of the Coulomb energy. In the resolution of the identity

  0947-6539/99/0501-0267 $ 17.50+.50/0

approach (RI), $\rho(r)$ is approximated by an expansion in atom-centered auxiliary basis sets [Eq. (1)] which avoids the evaluation of four-center two-electron integrals.[38]

$$\rho(r) \approx \sum_{\alpha} c_{\alpha}\alpha(r) = \tilde{\rho}(r) \quad (1)$$

The RI-DFT approach reduces, depending on the size of the molecule, the computational costs by a factor of four to ten.[38] In this work, the molecular structures of the isomers and transition states have been optimized at the RI-DFT level with the Becke–Perdew (B–P) parametrization[39] as implemented in TURBOMOLE.[40]

Accurate values for the isomer and transition-state energies have been obtained by performing single-point second-order Møller–Plesset (MP2) calculations. Computational savings of one order-of-magnitude without any loss of accuracy, when compared with conventional MP2 calculations, can be achieved by the use of auxiliary basis sets to short-cut the evaluation of two-electron integrals.[41–43]

The molecular structures of the transition states were obtained by fixing one R_{NH} bond length and optimizing all other degrees of freedom. This procedure was repeated for a number of R_{NH} and the stationary point was obtained by interpolation. The final energies of the transition states were obtained by optimizing the molecule with the interpolated R_{NH} bond length fixed and all the other degrees of freedom fully optimized.

Due to the large size of the molecule it was not possible to check whether the found minima and transition points are true minima and saddle points, respectively. The zero-point energies (ZPE) were assumed to be of the same order of magnitude as obtained at the semiempirical level for unsubstituted porphyrins.

The present RI-MP2 calculations are approximatively as time consuming as the Hartree–Fock calculation. For smaller systems the RI-MP2 calculations are often even faster than the corresponding Hartree–Fock calculation. A single-point RI-MP2 calculation on bonellin-dimethylester takes approximatively 20 hours of CPU time on a DEC Alpha 500/500 MHz workstation. All semiempirical calculations were performed on a 133 MHz Pentium PC with the HYPERCHEM program package, version 5.01.[44]

Basis sets: In this study we employed split-valence basis sets augmented with polarization functions. The sp parts (s part for hydrogen) of the basis sets were optimized for atoms at the self-consistent field (SCF) level.[45, 46] Two different basis sets were employed. The molecular optimizations were performed at DFT level with split-valence-quality basis set augmented with polarization functions on C, N, and O.[47] This basis set is denoted SV(P). However, in the final single-point DFT, SCF, and MP2 calculations, the basis set was augmented with polarization functions on H. The larger basis set we denote SVP. The exponents of the polarization functions were 0.8, 0.8, 1.0, and 1.2 for H, C, N, and O, respectively. In calculations of nuclear magnetic shielding constants for unsubstituted free-base *trans*-porphyrin and pyrrole, triple-zeta-quality basis sets augmented with polarization functions (TZVP) were employed.[48]

Different auxiliary basis sets were used in the RI-MP2 and RI-DFT calculations. In the RI-MP2 calculations, the auxiliary basis sets are constructed by decontracting the standard triple-zeta-quality basis sets[46, 48] and augmenting them with higher angular-momentum functions. The RI-MP2 auxiliary basis set for H consisted of 5s2p1d contracted to 3s2p1d (5s2p1d/3s2p1d), while for C, N and O we used 11s6p2d1f/6s4p2d1f auxiliary basis-sets. The optimized auxiliary basis sets used in the RI-DFT calculations[46] consisted of 4s2p/2s1p for H and of 8s3p3d1f/6s3p3d1f for C, N, and O.

The SV(P) basis set for bonellin-dimethylester resulted in 650 spherical Gaussians, while the SVP basis-set consisted of 764 spherical Gaussian basis functions. In the MP2 calculations, the core orbitals ($1s_C$, $1s_N$, and $1s_O$) were uncorrelated, which yielded 214 correlated electrons and 616 virtual orbitals, and since the calculations were performed in C_1 symmetry, the number of MP2 amplitudes became formally 4.3×10^9.

Results and Discussion

The structures of the six isomers of bonellin-dimethylester obtained by permuting the two inner hydrogens are shown in Figure 1. The migration paths between the isomers are schematically shown in Figure 2. For the discussion of the results the numbering scheme for the most relevant atoms is given in Figure 3. The pyrrole rings are numbered clockwise starting from the pyrrole ring with N^1. Since most computational studies of substituted porphyrins have so far been performed at semiempirical and molecular mechanical levels of theory, the energies and structures are compared with semiempirical values. The most significant differences between present DFT, MP2, and semiempirical values are emphasized.

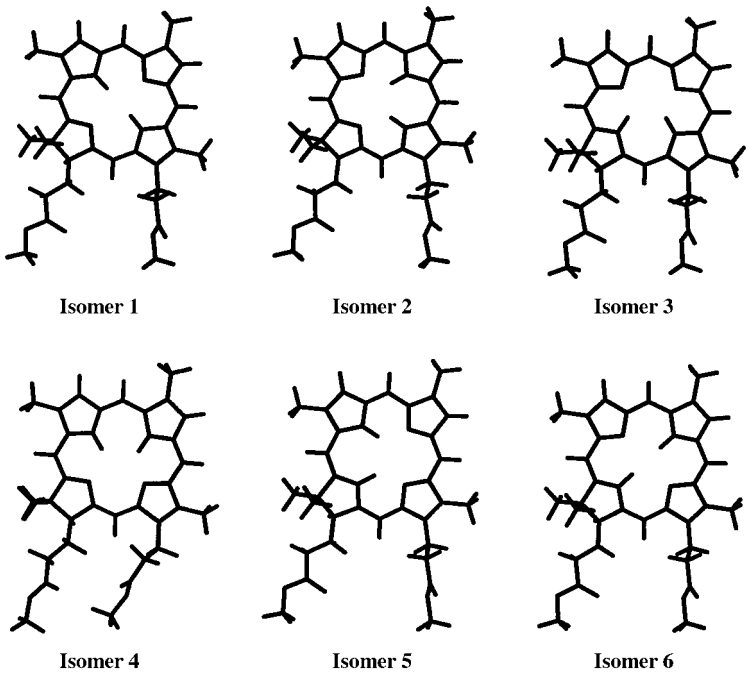

Figure 1. The optimized molecular structures of isomers **1** to **6**.

$$\begin{array}{ccccc} \mathbf{6} & \longleftrightarrow & \mathbf{2} & \longleftrightarrow & \mathbf{6} \\ \updownarrow & & \updownarrow & & \updownarrow \\ \mathbf{3} & \longleftrightarrow & \mathbf{1} & \longleftrightarrow & \mathbf{4} \\ \updownarrow & & \updownarrow & & \updownarrow \\ \mathbf{6} & \longleftrightarrow & \mathbf{5} & \longleftrightarrow & \mathbf{6} \end{array}$$

Figure 2. Transition paths between isomers of bonellin-dimethylester.

A. Energetics: The relative energies of the bonellin-dimethylester isomers are given in Table 1. Isomer 1, which is the energetically lowest isomer, is chosen to be the reference

0947-6539/99/0501-0268 $ 17.50+.50/0 *Chem. Eur. J.* **1999**, *5*, No. 1

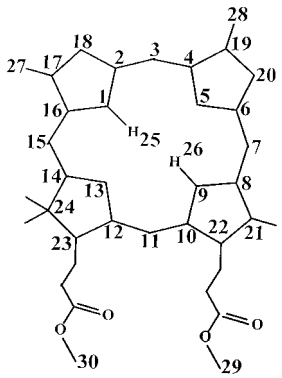

Figure 3. Numbering scheme for the atoms.

structure. As seen in Table 1, the isomer energies calculated at DFT level are 2–5 kcal mol^{-1} smaller than MP2 energies, while the SCF energies are at most 1 kcal mol^{-1} smaller than MP2 values except for isomer **6**, whose energy at Hartree–Fock level is 7 kcal mol^{-1} too large compared with the MP2 value. Calculations at semiempirical unrestricted Hartree–Fock (UHF) AM1[49] and PM3[50] levels provide approximately the same energy differences between the isomers as obtained at MP2 level. Since Crossley et al.[8] found in their NMR study of 5,10,15,20-tetraphenylporphyrins that the electronic structure of the substituents did not significantly affect the transition barriers, we did not consider it necessary to study the effect of different conformations of the side chains on the isomer and transition energies.

Table 1. The total energy of isomer **1** (in au) and isomer energies (in kcal mol^{-1}) relative to isomer **1** calculated at DFT, SCF, MP2, PM3, and AM1 levels of theory.

	Basis set	**1**	**2**	**3**	**4**	**5**	**6**
DFT	SV(P)	–1799.081780	5.90	13.66	5.41	13.29	6.39
DFT	SVP	–1799.170417	5.39	13.03	4.69	12.68	6.36
SCF	SVP	–1787.673624	8.92	16.90	8.52	16.25	1.99
MP2	SVP	–1793.542316	9.06	16.56	7.64	17.29	9.00
UHF PM3[a]		–	7.01	17.72	7.03	17.56	11.36
UHF AM1[a]		–	6.33	17.35	6.06	17.15	9.59

[a] By courtesy of Juho Helaja.[37]

As seen in Table 1, isomer **4** is at MP2 level 7.6 kcal mol^{-1} above isomer **1**, while isomers **2** and **6** are 9 kcal mol^{-1} above **1**. Isomers **3** and **5** are both significantly (16–17 kcal mol^{-1}) higher in energy than the other isomers.

Unsubstituted porphyrin with the inner hydrogens in *trans* position have been found to be energetically lower than *cis*-porphyrin.[4, 5, 29, 30] For bonellin-dimethylester there are two nondegenerate *trans*-isomers (isomer **1** and **6**). Isomer **1** is lower in energy, since its aromatic resonance pathway is not affected by the substituents. For isomer **6**, the two methyl groups connected to C^{24} destroy the aromatic resonance pathway of the porphyrin nucleus; this is also reflected in the bond lengths. In all isomers, the C_α–C_β bonds in the fourth pyrrole ring are 5–10 pm longer than the C_α–C_β bonds of the other pyrrole rings. The C_β–$C_{\beta'}$ bonds are 15–20 pm longer than the corresponding bonds of the other pyrrole rings (see Table 2). Isomers **2** and **4** with the inner hydrogens in *cis* position lie lower in energy than isomers **3** and **5**, since their resonance pathways are not affected by the two methyl groups at C^{24}. The aromaticity of the porphyrin nucleus and the aromatic resonance pathways of the isomers will be discussed in section C.

Table 2. The skeleton bond distances of the pyrrole rings[a] (in pm) as obtained for isomer **1**. The bond lengths are reported clockwise for each ring.

	N_α–C_α	C_α–C_β	C_β–$C_{\beta'}$	$C_{\beta'}$–$C_{\alpha'}$	$C_{\alpha'}$–N
Ring 1	137.4	145.2	138.9	143.8	138.3
Ring 2	137.2	147.3	137.5	146.0	137.0
Ring 3	138.4	144.8	139.6	145.0	137.2
Ring 4	135.8	153.8	156.7	154.7	135.6

[a] The pyrrole rings are numbered clockwise starting from the pyrrole ring with N^1.

The same rule can also be applied for the transition states. The transition state between isomers **1** and **2** ($TS_{1\leftrightarrow2}$) and $TS_{1\leftrightarrow4}$ are the lowest transition states, since they do not involve any hydrogens connected to N^{13}. The energies of the other transition states are considerable higher in energy. The energies of the transition states calculated at DFT level are all 3–7 kcal mol^{-1} too small, while the SCF energies are about 6–8 kcal mol^{-1} too large when compared with the MP2 values (see Table 3). At semiempirical level (UHF PM3) similar energies (ca. 29 kcal mol^{-1}) are obtained for both the $TS_{1\leftrightarrow2}$ and $TS_{1\leftrightarrow5}$ transition barriers; this is not in agreement with MP2 results. The reason for the discrepancy might be the fact that HYPERCHEM[44] was not able to find a true transition state; instead the PM3 calculations located hill tops on the energy surface with two imaginary frequencies. This finding might indicate an asynchronous hydrogen migration.[4] Alternatively semiempirical methods within HYPERCHEM are unable to provide reliable energy barriers for the hydrogen migration. Asynchronicity for the migration of hydrogens 25 and 26 (see Figure 3) was also indicated by the way the DFT optimization of the transition states was done. Since all other

Table 3. The energy barriers (in kcal mol^{-1}) of the transition states relative to isomer **1** calculated at DFT, SCF, MP2, and PM3 levels of theory.

	Basis set	$TS_{1\leftrightarrow2}$	$TS_{1\leftrightarrow3}$	$TS_{1\leftrightarrow4}$	$TS_{1\leftrightarrow5}$	$TS_{2\leftrightarrow6}$	$TS_{3\leftrightarrow6}$	$TS_{4\leftrightarrow6}$	$TS_{5\leftrightarrow6}$
DFT	SV(P)	10.0	15.2	9.7	15.5	14.5	16.4	13.9	16.7
DFT	SVP	9.3	14.2	8.8	14.8	13.7	15.3	12.9	15.9
SCF	SVP	22.9	29.0	22.8	28.6	26.8	30.4	26.2	29.7
MP2	SVP	13.5	20.8	12.1	20.8	20.6	18.7	18.3	21.6
MP2 + ZPE	SVP	8.5	15.8	7.1	15.8	15.6	13.7	13.3	16.6
UHF PM3		29.0	–	–	29.5	–	–	–	–

degrees of freedom were relaxed except the H–N distance of the migrating hydrogen, a synchronous motion of the other hydrogen would have been noted.

The difference in zero-point energy for unsubstituted *cis*-porphyrin relative to *trans*-porphyrin have previously been calculated at PM3 level to be -1 kcal mol^{-1},[5] while the ZPE contribution to the activation barrier at PM3 level is -5 kcal mol^{-1}.[5] The estimated zero-point energy corrected activation energies given in Table 3 are obtained by adding a ZPE contribution of -5 kcal mol^{-1} to the MP2 results.

In their calculation on PorH$^-$, Vangberg and Ghosh[7] found an activation barrier of 12.0 kcal mol^{-1} which is 4.7 kcal mol^{-1} lower than the activation barrier obtained for $PorH_2$.[5] However, since the $PorH_2$ energies were calculated at MP2 level,[5] while PorH$^-$ was studied at DFT level[7] the difference, which is of the same size as obtained for bonellin-dimethylester, is probably due to the fact that DFT calculations provide somewhat lower activation barriers than MP2 calculations. At DFT level polarization functions at the hydrogens reduce the energy differences between the isomers by 0.0–0.7 kcal mol^{-1} and the energy barriers by 0.7–1.1 kcal mol^{-1}.

B. Structures: The superposition of isomer **1** optimized at DFT level and at semiempirical UHF PM3 level, respectively, showed that the ring structures are almost identical whereas the flexible side chains differ slightly in their orientations. A notable difference between the semiempirical structures of the other isomers and those found at the DFT level is that the N–N distances differ considerably for all isomers except **1** and **6**. For isomers **1** and **6**, the superposition of the DFT and semiempirical structures yields an RMS deviation of the order 0.4 pm, whereas for the other isomers the deviation is about an order of magnitude larger. Where DFT finds strong deformation of the porphyrin skeleton, semiempirical methods largely underestimate this deformation.

The proton migration is strongly coupled to deformation of the porphyrin skeleton. The deformation can be illustrated by the N–N distances. As seen in Table 4, the distances between the nitrogens depend on the position of the inner hydrogen atoms. For isomer **1**, the distance between N^1 and N^5 is 294 pm. For isomer **2**, it is 270 pm (290 pm semiempirically), while for the transition state between the two isomers the $R_{N^1N^5}$ distance is only 252 pm. Generally, for *cis* isomers the distance between the pyrrole nitrogens, to which the inner hydrogens are connected, is up to 50 pm longer than the distance to the two adjacent nitrogens without hydrogens; this reflects the size of the hydrogens inside the ring. The distance between the nitrogens without any hydrogens is about as large as the distance between the nitrogens with the inner hydrogens (see Table 4).The porphyrin skeleton remains approximately planar for all the isomers and transition states. A qualitative look at the semiempirically calculated IR normal modes indicates that although the lowest frequency modes may be assigned to motion of atoms in the side chains, low-frequency modes exist that translate into breathing modes of the porphyrin skeleton. These modes increase the N–N distances and open up the meso angles.

Table 4. Distance between nitrogen atoms (in pm) for bonellin-dimethylester isomers and transition states.

	$R_{N^1N^5}$	$R_{N^1N^{13}}$	$R_{N^5N^9}$	$R_{N^9N^{13}}$
1	294.0	301.4	294.9	302.1
2	269.6	321.2	326.7	277.0
3	319.4	269.6	268.3	334.9
4	326.6	276.7	270.0	321.8
5	267.2	334.8	320.2	269.9
6	294.7	299.5	296.4	298.8
$TS_{1\leftrightarrow2}$	252.1	331.2	331.1	271.7
$TS_{1\leftrightarrow3}$	328.2	254.3	263.2	339.8
$TS_{1\leftrightarrow4}$	331.1	271.3	252.3	331.8
$TS_{1\leftrightarrow5}$	262.8	338.9	328.4	254.4
$TS_{2\leftrightarrow6}$	263.7	332.1	333.3	254.0
$TS_{3\leftrightarrow6}$	328.6	265.5	251.7	339.5
$TS_{4\leftrightarrow6}$	333.1	254.0	264.1	332.7
$TS_{5\leftrightarrow6}$	251.4	338.9	328.7	265.7

In Table 5, the C_α-C_{meso}-C_α bond angles are given. The values of the angles vary between 121° and 133° depending on the position of the inner hydrogens. This flexibility of the porphyrin nucleus causes large movements of the ester groups. Such cooperative movement may not be unimportant in biosystems. For isomer **4**, the distance between the end carbons of the ester groups (C^{29} and C^{30}) is only 517 pm, while for isomer **1** the distance is 769 pm and for the $TS_{1\leftrightarrow2}$ it is 863 pm (see the last column of Table 5). Ghosh and Almlöf[6] found significant differences for unsubstituted porphyrin in the C_α-C_{meso}-C_α bond angles for *cis* and *trans* porphyrin. The C_α-N-C_α angles have previously been found to be significantly wider in the N-protonated pyrrole rings[6] and this is often used for experimental determination of the connectivity of the inner hydrogens.

Table 5. The C_α-C_{meso}-C_α bond angles (in degrees) and the distance between the end carbons of the ester groups (in pm) for bonellin-dimethylester isomers and transition states.

	C^2-C^3-C^4	C^6-C^7-C^8	C^{10}-C^{11}-C^{12}	C^{14}-C^{15}-C^{16}	$R_{C^{29}C^{30}}$
1	127.3	127.7	129.0	128.7	768.7
2	123.7	132.1	125.2	132.4	838.9
3	131.7	124.0	134.1	123.8	678.9
4	132.0	123.8	132.6	125.0	516.9
5	123.7	131.9	123.9	133.9	852.0
6	127.5	127.8	128.3	128.3	750.7
$TS_{1\leftrightarrow2}$	121.1	132.9	124.2	133.8	863.2
$TS_{1\leftrightarrow3}$	132.8	123.1	135.0	121.5	500.9
$TS_{1\leftrightarrow4}$	132.9	121.1	134.1	124.1	509.5
$TS_{1\leftrightarrow5}$	122.9	133.1	121.5	134.7	869.8
$TS_{2\leftrightarrow6}$	122.9	133.5	121.4	133.9	869.6
$TS_{3\leftrightarrow6}$	133.0	121.3	134.9	123.1	503.0
$TS_{4\leftrightarrow6}$	133.2	122.9	134.1	121.4	496.8
$TS_{5\leftrightarrow6}$	121.3	133.0	123.2	134.7	852.8

For N-protonated pyrrole rings, the C_α-N-C_α bond angles of the first three pyrrole rings of the isomers are around 110°, while the angle for the fourth N-protonated pyrrole ring it is about 114° (see Table 6). The corresponding values for nonprotonated pyrrole rings are 105°–106° and 109°–111°. For transition states, the C_α-N-C_α bond angles of the partly protonated pyrrole rings are 106°–107° and 110°–111°, while the two remaining C_α-N-C_α angles are not significantly affected by the hydrogen migration. The fourth pyrrole ring

0947-6539/99/0501-0270 $ 17.50+.50/0 *Chem. Eur. J.* **1999**, *5*, No. 1

Table 6. The C_α-N-C_α bond angles (in degrees) for bonellin-dimethylester isomers and transition states.

	C^{16}-N^1-C^2	C^4-N^5-C^6	C^8-N^9-C^{10}	C^{12}-N^{13}-C^{14}
1	110.8[a]	105.3	110.8[a]	109.1
2	106.1	110.3[a]	110.4[a]	109.8
3	105.8	106.1	110.2[a]	114.0[a]
4	110.5[a]	110.4[a]	106.0	109.9
5	110.3[a]	106.1	105.8	114.0[a]
6	105.3	110.6[a]	105.2	114.5[a]
$TS_{1\leftrightarrow2}$	107.0	107.1	110.6[a]	109.9
$TS_{1\leftrightarrow3}$	106.4	106.3	110.4[a]	111.3
$TS_{1\leftrightarrow4}$	110.6[a]	107.1	106.9	109.9
$TS_{1\leftrightarrow5}$	110.5[a]	106.2	106.4	111.1
$TS_{2\leftrightarrow6}$	106.3	110.5[a]	106.4	110.8
$TS_{3\leftrightarrow6}$	105.9	107.0	107.2	114.3[a]
$TS_{4\leftrightarrow6}$	106.4	110.6[a]	106.2	111.0
$TS_{5\leftrightarrow6}$	107.4	106.9	105.9	114.2[a]

[a] An inner hydrogen is connected to the nitrogen.

behaves differently, since it has two methyl groups connected to C^{24} which actually makes it nonaromatic.

As seen in Table 7, the pyrrole structures optimized at DFT and MP2 levels are relatively similar for $PorH_2$[5, 6, 43] and $PorH^-$,[7] and for the DFT structure of bonellin-dimethylester

Table 7. Comparison of the pyrrole structure of bonellin-dimethylester with those of unsubstituted porphyrins (in pm). Only the three aromatic rings are considered.

	Method	N–C_α	C_α–C_β	C_β–C_β	C_α–C_{meso}
1	DFT/SV(P)[a]	137.1 ± 1.5	145.4 ± 1.5	138.7 ± 1.2	140.6 ± 0.8
$TS_{1\leftrightarrow2}$	DFT/SV(P)[a]	137.3 ± 2.4	145.3 ± 2.2	138.5 ± 1.1	140.6 ± 1.0
2	DFT/SV(P)[a]	137.1 ± 1.7	145.5 ± 3.0	138.7 ± 1.3	140.8 ± 1.1
$TS_{1\leftrightarrow4}$	DFT/SV(P)[a]	137.3 ± 2.3	145.4 ± 2.4	138.5 ± 0.5	140.6 ± 0.7
4	DFT/SV(P)[a]	137.1 ± 1.7	145.6 ± 3.1	138.6 ± 0.8	140.8 ± 1.2
trans-$PorH_2$	DFT/DNP[b]	136	142	137	139
cis-$PorH_2$	DFT/DNP[b]	137	143	137	139
trans-$PorH_2$	SCF/DZ(P)[c]	134.6	146.1	134.5	138.9
$PorH^-$	DFT/TZDP[d]	138	143	137	140
PorH-TS	DFT/TZDP[d]	138	144	137	140
trans-$PorH_2$	MP2/SVP[e]	136.8	143.6	137.9	139.9

[a] This work. Average value including maximum deviation. [b] Ref. [6]. [c] Imposed D_{2h} symmetry. No polarization functions on C.[5] [d] Ref. [7]. [e] Ref. [43]

isomers. Since the structures of the pyrrole units differ slightly, the average bond lengths of the pyrroles and the maximum deviation from the average values are given in Table 7. The fourth pyrrole ring is not considered in the bond-length averages. Though the deviations from the average values are up to 3 pm, the averages are remarkable equal for the isomers and transition states. At SCF level $PorH_2$ possesses a symmetry-broken structure with alternating bonds,[43, 51–53] while symmetry-imposed (D_{2h}) SCF calculations result in a pyrrole structure in which the bond lengths differ by ± 3 pm from MP2 values.[5] The isomers with one inner hydrogen connected to the fourth pyrrole ring have alternating bond lengths that indicates that the aromatic pathway is, at least partly, destroyed. The C_α–C_{meso} distances are given in Table 8.

The NH bond lengths (Table 9) for the *trans* isomers are 2–3 pm shorter than for the *cis* isomers or for the nonmigrating hydrogen of the transition states. The structures of the

Table 8. C_α–C_{meso} bond lengths for bonellin-dimethylester isomers (in pm).

	$R_{C^2C^3}$	$R_{C^3C^4}$	$R_{C^6C^7}$	$R_{C^7C^8}$	$R_{C^{10}C^{11}}$	$R_{C^{11}C^{12}}$	$R_{C^{14}C^{15}}$	$R_{C^{15}C^{16}}$
1	140.1	141.2	141.4	140.0	141.2	140.0	140.2	141.0
2	140.7	140.9	141.0	140.1	141.1	140.4	140.1	141.9
3	140.2	141.7	141.1	140.5	142.4	138.6	138.3	142.9
4	140.4	140.7	141.1	140.5	142.0	140.1	140.4	141.1
5	140.7	140.9	142.0	140.0	142.9	138.3	138.6	142.3
6	140.2	140.9	141.2	139.9	142.8	138.2	138.2	142.8

Table 9. Distance between N–H for bonellin-dimethylester isomers and transition states (in pm).

	$R_{N^1H^{25}}$	$R_{N^5H^{25}}$	$R_{N^9H^{25}}$	$R_{N^{13}H^{25}}$	$R_{N^1H^{26}}$	$R_{N^5H^{26}}$	$R_{N^9H^{26}}$	$R_{N^{13}H^{26}}$
1	102.9	228.5	322.5	242.9	322.6	228.7	102.9	243.9
2	185.3	105.4	286.3	332.6	318.1	282.9	104.0	199.7
3	182.8	330.8	293.4	106.7	320.5	184.5	105.5	296.9
4	104.1	283.9	317.2	199.2	285.0	105.3	186.2	334.0
5	105.7	183.0	321.5	297.0	293.4	330.0	183.3	106.6
6	229.9	103.2	233.4	331.4	234.3	330.8	233.2	103.8
$TS_{1\leftrightarrow2}$	135.6	128.3	318.9	325.3	322.5	284.4	104.0	194.4
$TS_{1\leftrightarrow3}$	140.8	326.4	319.0	125.8	323.2	178.5	105.7	301.1
$TS_{1\leftrightarrow4}$	104.0	285.5	321.4	193.9	318.0	128.5	135.6	326.5
$TS_{1\leftrightarrow5}$	105.8	178.1	324.7	299.4	319.7	324.5	140.8	125.9
$TS_{2\leftrightarrow6}$	179.8	105.4	289.3	334.5	313.9	328.7	135.2	131.0
$TS_{3\leftrightarrow6}$	316.0	135.6	128.2	329.7	178.3	334.6	295.4	106.9
$TS_{4\leftrightarrow6}$	287.7	105.3	180.7	336.4	135.2	330.2	312.8	131.0
$TS_{5\leftrightarrow6}$	127.9	135.6	317.4	328.0	295.5	332.7	178.8	106.8

transition state can be explained by applying Hammonds postulate.[54] For example in $TS_{1\leftrightarrow2}$, the migrating hydrogen is closer to N^5 than to N^1, that is, the structure of the transition state is closer to **2** than to **1**. This is quite easy to understand by assuming a simple quadratic model for the potential curve close to the minimum of the isomers, and noting that **1** is below **2** in energy. The same rule can be applied to explain the structure of the transition states between the other isomers.

The complete molecular structures of the isomers and transition states including internal coordinates can be found on the internet page, ftp.chem.helsinki.fi/pub/people/sundholm/bonellin.

C. Nuclear magnetic shieldings: Nuclear magnetic shieldings have been calculated at Hartree–Fock level[55] with SVP basis sets. The absolute shieldings for the inner and outer hydrogens are given in Table 10. For comparison, the absolute shieldings of pyrrole and unsubstituted free-base *trans*-porphyrin have been calculated at Hartree–Fock level with triple-zeta

Table 10. The absolute nuclear magnetic shieldings for the inner and outer hydrogens of the six isomers (in ppm).

	1	**2**	**3**	**4**	**5**	**6**
N^1–H	34.8	–	–	32.6	25.5	–
N^5–H	–	30.6	–	30.4	–	28.0
N^9–H	34.9	33.2	26.0	–	–	–
N^{13}–H	–	–	26.6	–	26.6	29.5
C^3–H	21.8	22.7	23.2	22.2	22.8	23.4
C^7–H	21.9	22.1	22.8	22.9	23.3	23.4
C^{11}–H	23.2	23.4	24.4	23.3	24.4	24.6
C^{15}–H	23.4	23.6	24.4	23.6	24.6	24.7
C^{18}–H	22.4	22.9	23.2	22.5	23.3	23.4
C^{20}–H	23.0	22.8	23.5	23.3	24.0	23.9

valence-quality basis sets augmented with polarization functions (TZVP).[48] The absolute shielding for the inner hydrogens of *trans* porphyrin is 39.7 ppm. For the outer hydrogens the obtained shieldings are about 21 – 22 ppm. The correlation contribution to the shieldings of the inner hydrogens obtained at MP2 level [56, 57] with the SV(P) basis sets is −2.6 ppm, yielding an extrapolated MP2 value of 37.1 ppm for the inner hydrogens of *trans* porphyrin. The large value for the shielding of the inner hydrogens is due to the induced ring current in the aromatic pathway. The shieldings of the outer hydrogens are significantly smaller, since they lie outside the conducting ring system. For pyrrole, the absolute shielding of the NH hydrogen calculated at Hartree – Fock level is 24.5 ppm, while at MP2 level the obtained shielding is 24.0 ppm. In the shielding calculations on pyrrole the TZVP basis sets were employed.

Possibly the nuclear independent chemical shifts (NICS)[58, 59] correlate with ring aromaticity, but the obtained NICS values for unsubstituted *trans* porphyrin do not prove that the NH units are integral parts of the aromatic pathway as recently suggested by Cyrañski et al.[60] The observation that the pyrrole rings with the inner hydrogens have larger NICS values than the two remaining ones may be due to the fact that three of their bonds belong to the aromatic pathway, while only two bonds of the two other pyrrole rings incorporate this path. Since the fourth pyrrole ring of bonellin-dimethylester is nonaromatic, the position of the inner hydrogen significantly affects the aromatic pathway of the porphyrin nucleus. At the fourth pyrrole ring, the aromatic pathway is forced to take the inner route regardless of the position of the inner hydrogens. The lowest isomer (**1**) and isomers **2** and **4** have no hydrogen connected to the nitrogen of the fourth pyrrole ring. As seen in Table 10, for isomers **1**, **2** and **4**, the shieldings of the inner hydrogens are larger than 30 ppm indicating the existence of an aromatic pathway around the porphyrin nucleus analogous to that of unsubstituted free-base *trans* porphyrin. For isomers **3** and **5**, which are *cis* isomers with one inner hydrogen connected to the fourth pyrrole ring (N^{13}), the shieldings of the inner hydrogens are about 25 – 26 ppm indicating the absence of an aromatic pathway around the porphyrin nucleus. Hydrogen shieldings of 25 – 26 ppm are typical for unsaturated, nonaromatic hydrocarbons. For all isomers with an inner hydrogen connected to the fourth pyrrole ring, the C_α–C_{meso} bonds on both sides of the fourth pyrrole ring alternate (see Table 8), showing that the aromatic resonance is weaker or even absent. For isomers with an inner hydrogen connected to N^{13}, the shieldings of the outer hydrogens are always larger than for the other isomers indicating a weaker aromaticity for these isomers. Note that isomers **3** and **5** are the energetically highest isomers. Finally, isomer **6** has the inner hydrogens in *trans* position and one of them is connected to N^{13}. Their shieldings are 28.0 and 29.5 ppm, respectively, which must be considered to be outside the aromatic range.

Judging from these observations we conclude that the preferred aromatic pathway does not include the NH bridge as recently suggested by Cyrañski et al;[60] instead a classical [18]annulene structure is formed, with the NH groups as relatively inert bridging units. The carbon and nitrogen shieldings did not provide any easily interpretable information about the aromatic pathways.

Conclusions

- The molecular structures for six bonellin-dimethylester isomers and the transition states of the inner-hydrogen migration have been optimized at DFT level with SV(P)-quality basis sets.
- Accurate values for the energies of the isomers and transition states have been calculated at MP2 level with the DFT structures and SVP-quality basis sets.
- The lowest isomer (isomer **1**) has the inner hydrogens connected in the *trans* position to N^1 and N^9.
- A hydrogen at N^{13} destroys the aromatic π-electron pathway resulting in high-energy isomers and transition states.
- The second isomer with the inner hydrogen in the *trans* position (isomer **6**) is 9 kcal mol^{-1} above isomer **1**, since the two methyl groups connected to C^{24} prevent the aromatic pathway from taking take the outer route at the fourth pyrrole ring.
- Isomers **3** and **5** lie high in energy since they both are *cis* isomers with a hydrogen connected to N^{13}.
- The transition states $TS_{1\leftrightarrow3}$, $TS_{1\leftrightarrow5}$, $TS_{2\leftrightarrow6}$, $TS_{3\leftrightarrow6}$, $TS_{4\leftrightarrow6}$, and $TS_{5\leftrightarrow6}$ lie significantly higher in energy than $TS_{1\leftrightarrow2}$ and $TS_{1\leftrightarrow4}$, since they all have a hydrogen connected to N^{13}.
- The hydrogen migration is found to involve a significant deformation of the porphyrin skeleton mainly through a change in the bond angle at C_{meso}.
- The distance between the ester groups of the side chains depends strongly on the positions of the inner hydrogens.
- The porphyrin skeleton remains approximatively planar for all isomers and transition states.
- The present calculations of nuclear magnetic shielding constants do not support the recent notion that the inner NH groups are integral parts of the aromatic pathway in porphyrins.[60] It therefore seems as if the traditional [18]annulene picture of the porphyrin nucleus still holds.

Acknowledgements

The authors are grateful to Professor P. Hynninen and J. Helaja for attracting our attention to the problem of the bonellin tautomers and for providing semiempirical bonellin-dimethylester structures prior to publication. We also thank Professor F.-P. Montforts from whose laboratory the bonellin-dimethylester originated. Finally we thank Professor R. Ahlrichs for a recent version of TURBOMOLE. This work has been supported by grants from The Academy of Finland.

[1] J. Braun, C. Hasenfratz, R. Schwesinger, H. H. Limbach, *Angew. Chem.* **1994**, *106*, 2302; *Angew. Chem. Int. Ed. Engl.* **1994**, *33*, 2215 – 2217.
[2] J. Braun, H. H. Limbach, P. G. Williams, H. Morimoto, D. E. Wemmer, *J. Am. Chem. Soc.* **1996**, *118*, 7231.
[3] J. Braun, M. Schlabach, B. Wehrle, M. Köcher, E. Vogel, H.-H. Limbach, *J. Am. Chem. Soc.* **1994**, *116*, 6593.
[4] K. M. Merz, C. H. Reynolds, *J. Chem. Soc. Chem. Commun.* **1988**, 90.

  0947-6539/99/0501-0272 $ 17.50+.50/0 *Chem. Eur. J.* **1999**, *5*, No. 1

[5] J. R. Reimers, T. X. Lü, M. J. Crossly, N. S. Hush, *J. Am. Chem. Soc*. **1995**, *117*, 2855.
[6] A. Ghosh, J. Almlöf, *J. Phys. Chem*. **1995**, *99*, 1073.
[7] T. Vangberg, A. Ghosh, *J. Phys. Chem. B* **1997**, *101*, 1496.
[8] M. J. Crossley, L. D. Field, M. M. Harding, S. Sternhell, *J. Am. Chem. Soc*. **1987**, *109*, 2335.
[9] M. J. Crossley, M. M. Harding, S. Sternhell, *J. Org. Chem*. **1992**, *57*, 1833.
[10] J. Baker, P. M. Kozlowski, A. A. Jarzecki, P. Pulay, *Theor. Chem. Acc*. **1997**, *97*, 59.
[11] M. Boronat, E. Ortí, P. M. Viruela, F. Tomas, *J. Mol. Struct. (THEOCHEM)* **1997**, *390*, 149.
[12] L. Kümmerl, H. Kliesch, D. Wöhrle , D. Haarer, *Chem. Phys. Lett*. **1994**, *227*, 337.
[13] A. Ghosh, T. Vangberg, *Theor. Chem. Acc*. **1997**, *97*, 143.
[14] A. Ghosh, J. Almlöf, P. G. Gassman, *Chem. Phys. Lett*. **1991**, *186*, 113.
[15] D. Lamoen, M. Parrinello, *Chem. Phys. Lett*. **1996**, *248*, 309.
[16] M. Noojien, R. J. Bartlett, *J. Chem. Phys.* **1997**, *106*, 6449.
[17] U. Nagashima, T. Takada, K. Ohno, *J. Chem. Phys*. **1986**, *85*, 4524.
[18] A. Ghosh, J. Almlöf, *Chem. Phys. Lett*. **1993**, *213*, 519.
[19] M. Merchán, E. Ortí, B. O. Roos, *Chem. Phys. Lett*. **1994**, *226*, 27.
[20] R. Bauernschmitt, R. Ahlrichs, *Chem. Phys. Lett*. **1996**, *256*, 454.
[21] X.-Y. Li, M. Z. Zgierski, *J. Phys. Chem.* **1991**, *95*, 4268.
[22] P. M. Kozlowski, M. Z. Zgierski, P. Pulay, *Chem. Phys. Lett*. **1995**, *247*, 379.
[23] P. M. Kozlowski, A. A. Jarzécki, P. Pulay, *J. Phys. Chem*. **1996**, *100*, 7007.
[24] P. G. Gassman, A. Ghosh, J.Almlöf, *J. Am. Chem. Soc*. **1992**, *114*, 9990.
[25] S. Rao, V. Krishnan, *J. Mol. Struct*. **1994**, *327*, 279.
[26] A. Ghosh, *J. Phys. Chem*. **1994**, *98*, 11004.
[27] A. Ghosh, *J. Mol. Struct. (THEOCHEM)* **1996**, *388*, 359.
[28] Z. Wang, P. N. Day, R. Pachter, *J. Chem. Phys.* **1998**, *108*, 2504.
[29] A. Ghosh, K. Jynge, *J. Phys. Chem. B* **1997**, *101*, 5459.
[30] A. Ghosh, *J. Phys. Chem. B* **1997**, *101*, 3290.
[31] C. R. Lederer, *Acad. Sci*. **1939**, *209*, 528.
[32] M. J. Gauthier, M. de Nicola-Giudici, *Curr. Microbiol*. **1983**, *8*, 195.
[33] R. F. Nigrelli, M. F. Stempien, G. D. Ruggieri, V. R. Liguori, J. T. Cecil, *Fed. Proc.* **1967**, *26*, 1197.
[34] P. Lallier, *C. R. Acad. Sci*. **1955**, *240*, 1489.
[35] F.-P. Montforts, C. M. Müller, A. Lincke, *Liebigs Ann. Chem*. **1990**, 415.
[36] F.-P. Montforts, U. M. Schwartz, *Liebigs Ann. Chem*. **1991**, 709.
[37] J. Helaja, F.-P. Montforts, I. Kilpeläinen, P. H. Hynninen, *J. Org. Chem.*, in press.
[38] K. Eichkorn, O. Treutler, H. Öhm, M. Häser, R. Ahlrichs, *Chem. Phys. Lett*. **1995**, *240*, 283.
[39] S. H. Vosko, L. Wilk, M. Nusair, *Can. J. Phys.* **1980**, *58*, 1200; J. P. Perdew, *Phys. Rev. B* **1986**, *33*, 8822; A. D. Becke, *Phys. Rev. B* **1988**, *38*, 3098.
[40] R. Ahlrichs, M. Bär, M. Häser, H. Horn, C. Kölmel, *Chem. Phys. Lett*. **1989**, *162*, 165.
[41] D. Feller, E. D. Glendening, D. E. Woon, M. W. Feyereisen, *J. Chem. Phys.* **1995**, *103*, 3526.
[42] M. W. Feyereisen, D. Feller, D. A. Dixon, *J. Phys. Chem*. **1996**, *100*, 2993.
[43] F. Weigend, M. Häser, *Theor. Chem. Acc*. **1997**, *97*, 143.
[44] HYPERCHEM, Hypercube, http://www.hyper.com.
[45] A. Schäfer, H. Horn, R. Ahlrichs, *J. Chem. Phys.* **1992**, *97*, 2571.
[46] The basis sets are available by FTP from host ftp.chemie.uni-karlsruhe.de (login-id: ftp) from directory pub/basis.
[47] T. H. Dunning, Jr., *J. Chem. Phys.* **1989**, *90*, 1007.
[48] A. Schäfer, C. Huber, R. Ahlrichs, *J. Chem. Phys.* **1994**, *100*, 5829.
[49] M. J. S. Dewar, E. G. Zoebisch, E. F. Healy, J. J. P. Stewart, *J. Am. Chem. Soc*. **1985**, *107*, 3902.
[50] J. J. P. Stewart, *J. Comp. Chem*. **1989**, *10*, 209; J. J. P. Stewart, *J. Comp. Chem*. **1989**, *10*, 221.
[51] J. Almlöf, T. H. Fischer, P. G. Gassman, A. Ghosh, M. Häser, *J. Phys. Chem*. **1993**, *97*, 10964.
[52] J. B. Foresman, M. Head-Gordon, J. A. Pople, M. J. Frisch, *J. Phys. Chem*. **1992**, *96*, 135.
[53] M. Merchán, E. Ortí, B. O. Roos, *Chem. Phys. Lett*. **1994**, *221*, 136.
[54] G. S. Hammond, *J. Am. Chem. Soc*. **1955**, *77*, 334.
[55] M. Häser, R. Ahlrichs, H. P. Baron, P. Weis, H. Horn, *Theoret. Chim. Acta* **1992**, *83*, 551.
[56] M. Kollwitz, J. Gauss, *Chem. Phys. Lett*. **1996**, *260*, 639.
[57] M. Kollwitz, J. Gauss, M. Häser, *J. Chem. Phys.* **1998**, *108*, 8295.
[58] P. von R. Schleyer, C. Maerker, A. Dransfeld, H. Jiao, N. J. R. van Eikema Hommes, *J. Am. Chem. Soc.* **1996**, *118*, 6317.
[59] G. Subramanian, P. von R. Schleyer, H. Jiao, *Angew. Chem*. **1996**, *108*, 2824; *Angew. Chem. Int. Ed. Engl*. **1996**, *35*, 2638.
[60] M. K. Cyrañski, T. M. Krygowski, M. Wisiorowski, N. J. R. van Eikema Hommes, P. von R. Schleyer, *Angew. Chem*. **1998**, *110*, 187; *Angew. Chem. Int. Ed.* **1998**, *37*, 177.

Received: February 6, 1998
Revised version: May 6, 1998 [F993]